Inhibition of Gene Expression and Cell Proliferation by Triple Helix-Forming Oligonucleotides Directed to the *c-myc* Gene[†]

Carlo V. Catapano,* Eileen M. McGuffie, Daniel Pacheco, and Giuseppina M. R. Carbone

Department of Experimental Oncology and Hollings Cancer Center, Medical University of South Carolina, Charleston, South Carolina 29425

Received September 21, 1999; Revised Manuscript Received February 11, 2000

ABSTRACT: Triple helix-forming oligonucleotides (TFOs) bind with high affinity and specificity to homopurine-homopyrimidine sequences in DNA and have been shown to inhibit transcription of target genes in various experimental systems. In the present study, we evaluated the ability of 3′-amino-modified phosphodiester TFOs directed to four sites in the *c-myc* gene to inhibit gene expression and proliferation of human leukemia (CEM, KG-1, and HL-60) and lymphoma (Raji and ST486) cells. GT-rich TFOs were designed to target sequences located either upstream (myc1 and -2) or downstream (myc3 and -4) of the P2 promoter, which is the major *c-myc* promoter. Myc2, which was directed to a site immediately upstream of this promoter, inhibited *c-myc* expression and proliferation of CEM cells. The effects of this TFO were sequence- and target-specific, since control oligonucleotides and TFOs directed to other sites were less or not active. Myc2 was also effective in KG-1, HL-60, and Raji cells. In contrast, ST486 cells were more sensitive to myc3, which targets a sequence in intron 1 upstream of the P3 promoter, than myc2. As result of a chromosomal translocation, P3 is the active promoter in ST486 cells. This study demonstrates the activity and specificity of TFOs designed to act as repressors of *c-myc* gene expression in human leukemia and lymphoma cells. Our results suggest that this is a valid approach to selectively inhibit gene expression and cancer cell growth, and encourage further investigation of its potential applications in cancer therapy.

The *c-myc* gene encodes a transcription factor that plays a critical role in controlling cell proliferation and differentiation (*1*). The *c-myc* gene product acts as a master switch that, in response to a variety of internal and external signals, either activates or represses transcription of several growth- and differentiation-related genes (*1*). c-Myc also has a key role in the pathogenesis and progression of several human cancers (*1*, *2*). Gene amplification, which leads to constitutive expression of *c-myc*, is observed frequently in cancers of the breast, lung, and prostate, and, occasionally, in colon carcinomas, leukemias, and lymphomas. Chromosomal translocations involving the *c-myc* gene are characteristics of Burkitt's lymphomas and frequently observed in a subgroup of AIDS-related lymphomas and leukemias. These translocations juxtapose the *c-myc* gene on chromosome 8 to the regulatory regions of immunoglobulin genes on chromosome 2, 14, or 22, and result in constitutive activation of *c-myc* gene expression (*3*). High levels of *c-myc* RNA and protein are also found in a large number of human cancers as a consequence of activation of other oncogenes, expression of products of chromosomal translocations, and alterations in tumor suppressor gene pathways (*1*, *2*).

The importance of deregulated expression of *c-myc* for proliferation of cancer cells and maintenance of the malignant phenotype has been demonstrated using various experimental approaches, including antisense oligonucleotides and c-Myc dominant negative mutants (*4*−*9*). In addition to providing essential information on the role of this gene in neoplastic transformation, these studies have suggested that targeting c-Myc is a valid approach to inhibit proliferation and survival of a variety of cancer cell types. Therefore, development of selective c-Myc inhibitors is of extreme interest, since such agents may have potential therapeutic applications in a wide range of human cancers.

The triplex DNA-based or antigene approach may provide an effective way to selectively inhibit the expression of a specific gene, such as *c-myc*, in cancer cells (*10*−*12*). Potential advantages of this approach are the limited number of target molecules per cell (i.e., gene copy number) and, perhaps, an increased level of selectivity compared to other oligonucleotide-based gene targeting strategies, such as antisense and decoy oligonucleotides. The triplex DNA approach is based on the design of oligonucleotides that bind in a sequence-specific manner to homopurine-homopyrimidine tracts in duplex DNA and can act as selective gene repressors. The third strand oligonucleotide forms a triple helix by interacting with the purine-rich strand of the duplex DNA via Hoogsteen hydrogen bonds (*13*, *14*). TFOs[1] can be oriented either parallel (pyrimidine motif) or antiparallel (purine motif) to the purine-rich strand of the duplex DNA (*10*−*12*). Antiparallel purine-rich TFOs have the advantage

[†] This work was supported in part by grants from the National Cancer Institute (CA70735), the American Medical Association−Education and Research Foundation, and the Medical University of South Carolina Institutional Research Funds (to C.V.C).

* To whom correspondence should be addressed at the Department of Experimental Oncology, Hollings Cancer Center, Medical University of South Carolina, 171 Ashley Ave., Charleston, SC 29425. Phone: (843) 792-6648. Fax: (843) 792-3200. E-mail: Catapanc@musc.edu.

10.1021/bi992185w CCC: $19.00
Published on Web 04/07/2000

over pyrimidine-rich TFOs that they form stable triple helices at physiological pH (*13*, *15*). Oligonucleotide-directed triplex DNA formation prevents binding of sequence-specific DNA binding proteins, such as transcription factors, to their target sequence (*16*, *17*). When directed to appropriate sites within the regulatory or transcribed region of a gene, TFOs can block transcription initiation or elongation of RNA transcripts (*11*). Several studies have confirmed the ability of TFOs to inhibit transcription in cell-free systems and expression of reporter genes in cells (*18*−*29*). Also, inhibition of the expression of various endogenous genes, including *c-myc*, by oligonucleotide-directed triplex DNA formation has been shown in cells (*30*−*37*). To date, however, only a limited number of studies have evaluated the ability of TFOs to inhibit cancer cell growth (*34*, *37*, *38*).

In this study, purine-rich TFOs were designed to target distinct sites in the *c-myc* gene. We selected sequences near critical control elements in the promoter and transcribed region of the gene, with the intent to inhibit *c-myc* gene expression by blocking either transcription initiation or elongation (Figure 1). The overall goal of the study was to compare the ability of these TFOs to down-regulate *c-myc* expression and inhibit growth of various human leukemia and lymphoma cell lines. Continuous expression of *c-myc* was known to be an important factor for proliferation and survival of these cells (*39*). Furthermore, the selected cell lines overexpressed *c-myc* because of either constitutive activation, gene amplification, or chromosomal translocation. Therefore, we were also in the position to determine whether the designed TFOs could affect cells with different mechanisms of activation of *c-myc* gene expression and, at the same time, could discriminate among cells with distinct alterations in the *c-myc* locus. Our studies showed the growth inhibitory activity of a TFO targeted to a site in the promoter of the *c-myc* gene in human leukemia CEM cells. The antiproliferative activity of this TFO depended on its ability to selectively down-regulate *c-myc* expression. Furthermore, the sensitivity of each cell line to distinct TFOs was apparently related to the presence and/or function of the corresponding target sequences in the *c-myc* regulatory region.

MATERIALS AND METHODS

Oligonucleotide Synthesis. Reagents for oligonucleotide synthesis were purchased from Glen Research (Sterling, VA). Phosphodiester oligonucleotides were synthesized by the phosphoroamidite method in the DNA synthesis facility of the Medical University of South Carolina. Oligonucleotides to be used for in vivo studies were modified at the 3′ terminus by addition of a propylamine group using 3′-amino-modifier CPG from Glen Research. Oligonucleotides were purified by preparative gel electrophoresis, dissolved in water, and sterilized by filtration through 0.22 μm filters (Gelman Science, Ann Arbor, MI). Oligonucleotide concentrations were determined spectrophometrically by measuring absorbance at 260 nm and using nucleotide extinction coefficients. Integrity and purity of the oligonucleotides were verified by gel electrophoresis.

Electrophoretic Mobility Shift Assay (EMSA). Oligonucleotides corresponding to the purine- and pyrimidine-rich strands of the target sequences shown in Figure 1 were synthesized. EMSA was performed according to two distinct protocols. In the experiments shown in Figure 2, the pyrimidine-rich strand of the target sequence was 5′ end-labeled with [γ-^{32}P]ATP (3000 Ci/mmol, Amersham Pharmacia Biotech, Piscataway, NJ) and T4 polynucleotide kinase (Promega, Madison, WI). To form duplex DNA, each end-labeled oligonucleotide was heated at 90 °C for 10 min in the presence of an equal amount of the complementary purine-rich oligonucleotide, and then allowed to cool slowly to room temperature. TFOs and control oligonucleotides were heated at 65 °C for 10 min to reduce self-aggregation. Then, duplex DNA (1 nM) was incubated with TFOs or control oligonucleotides in a buffer consisting of 90 mM Tris−borate (pH 8.0) and 10 mM $MgCl_2$ (TBM buffer) for either 1 or 18 h at 37 °C. An alternative protocol was used for the experiment shown in Figure 3. In this case, unlabeled duplex DNA was prepared by annealing the purine- and pyrimidine-rich oligonucleotides and then incubated with the TFO or control oligonucleotides, which had been 5′ end-labeled with [γ-^{32}P]ATP. To detect triplex DNA formation, binding reactions from both sets of experiments were subjected to polyacrylamide gel electrophoresis under nondenaturating conditions. Electrophoresis was carried out at room temperature at 600 V for 4 h using TBM as running buffer. The percentage of triplex DNA formed by the TFOs was determined by scanning the gels with a phosphoimager and using the Image-Quant software (Molecular Dynamics, Sunnyvale, CA). For each gel lane, we measured the intensity of the bands corresponding to the duplex and triplex DNA and calculated the percentage of duplex DNA that migrated as triplex DNA. The dissociation constant (K_d) for each TFO was then calculated using data from multiple experiments and the following equation: [duplex]/[triplex] = $K_d \times 1/[\text{TFO}]$ (*40*).

DNase I Footprinting. A fragment of 2000 bp comprising exon 1 of the *c-myc* gene was excised from the pHSR-1 plasmid (American Type Culture Collection, Manassas, VA) by digestion with *Xma*I and subcloned into a pGEM-3Z vector (Promega, Madison, WI). This plasmid was then digested with *Hin*dIII and *Ngo*MIV to generate a fragment of 347 bp containing the TFO target site. Following its isolation from an agarose gel using the Qiaex II kit (Qiagen, Valencia, CA), the fragment was labeled at the 3′ termini by filling in with the Klenow fragment of *E. coli* DNA polymerase I in the presence of [α-^{32}P]dCTP (3000 Ci/mmol, Amersham Pharmacia Biotech). To produce a fragment with the ^{32}P label only at the 3′ end of the strand containing the purine-rich target sequence, the 347 bp fragment was digested with *Xma*I. The resulting 314 bp fragment was subsequently purified by preparative gel electrophoresis. To carry out DNase I footprinting, TFO and control oligonucleotides were heated at 65 °C for 10 min, and then added to end-labeled DNA and incubated for 24 h at 37 °C in TBM buffer. DNase I (Promega) was added to the samples at a final concentration of 10 units/mL, and digestion was carried out for 1 min at

[1] Abbreviations: AML, acute myeloid leukemia; bp, base pair(s); CNBP, cellular nucleic acid-binding protein; DMS, dimethyl sulfate; EMSA, electrophoretic mobility shift assay; GAPDH, glyceraldehyde-3-phosphate dehydrogenase; hnRNP K, heterogeneous nuclear ribonucleoprotein K; MAZ, myc-associated zinc finger protein; MTT, 3-(4,5-dimethylthiazol-2-yl)-2,5-diphenyltetrazolium bromide; PBS, phosphate-buffered saline; RT-PCR, reverse transcriptase-polymerase chain reaction; SDS, sodium dodecyl sulfate; TCA, trichloroacetic acid; TFO, triple helix-forming oligonucleotide.

room temperature. Reactions were stopped by adding an equal volume of denaturating gel loading buffer containing 98% formamide and 10 mM EDTA, and heating for 10 min at 95 °C. Samples were loaded on a 10% sequencing gel and separated at 60 W for 2 h. An aliquot of the 314 bp fragment was sequenced with the SequiTherm Cycle sequencing system (Epicenter Technologies, Madison, WI) following the manufacturer's instructions and using a ^{32}P end-labeled primer (5′-GCCCGCTCGCTCCCTCTG-3′, nucleotides 2534−2517 of the *c-myc* gene) complementary to the 3′ end of the strand containing the purine-rich sequence. Sequencing reactions were then run in the gel along the side of the DNase I digests to identify the position of the target sequence.

Cell Culture Conditions and Oligonucleotide Treatment. Tissue culture medium, serum, and antibiotics were obtained from GIBCO/BRL. T-cell leukemia CEM cells were grown in E-MEM medium (*41*). KG-1 and Raji cells were obtained from D. Watson, and HL-60 cells were obtained from A. Safa of the Medical University of South Carolina. Burkitt's lymphoma ST486 cells were purchased from the American Type Culture Collection. KG-1, HL-60, Raji, and ST486 were grown in RPMI medium. Culture media were supplemented with 10% fetal calf serum that had been inactivated at 55 °C for 45 min. Before each experiment, cells were grown at a density of 2×10^5 cells/mL for 24 h and then diluted in fresh medium to the required cell density. Oligonucleotides were diluted to the desired concentrations and heated at 65 °C for 10 min immediately before being added to the culture medium to reduce the possibility of self-aggregation.

Thymidine Incorporation Assay. Measurements of the incorporation of radiolabeled thymidine into DNA were used to evaluate the effects of TFOs on cell proliferation. Cells were plated at a density of 5×10^4 cells/mL in 96-well plates and incubated with TFOs or control oligonucleotides. After 72 h, [^{3}H]thymidine (Moravek Biochemicals, Brea, CA) was added to a final concentration of 0.25 μCi/mL, and the cells were incubated for additional 24 h. At the end of this incubation, 50 μL aliquots of cell suspension were drawn from each well and spotted directly on GF/C filters (Whatman), which had been previously treated with 0.2 N NaOH. The filters were washed twice with 10 mL of an ice-cold 10% solution of TCA, and then in sequence with 10 mL of 5% TCA, water, and ethanol. The amount of radiolabeled thymidine incorporated into DNA was determined by liquid scintillation counting of the filters.

MTT Assay. Cells (100 μL/well of 96-well plates) were incubated with TFOs or control oligonucleotides for 96 h. Starting cell concentrations were 10 000 cells/mL for CEM cells, and 40 000 cells/mL for KG-1, HL-60, Raji, and ST486 cells. At the end of the 96 h incubation, 25 μL of MTT (5 mg/mL in PBS) was added to each well. After 4 h, 100 μL of a lysis buffer containing 20% SDS (w/v), 50% dimethylformamide (v/v), and 1% acetic acid (v/v) was added. After an overnight incubation at 37 °C, the absorbance was measured at 570 nm on a microplate reader. Three replicates were made for each treatment group, and each experiment was repeated at least twice.

Oligonucleotide Uptake and Intracellular Stability. The 3′-amino-modified oligonucleotide myc1A (Table 1) was 5′ end-labeled with [γ-^{32}P]ATP. Unincorporated [γ-^{32}P]ATP was removed by centrifugation through a Biospin 6 column (Bio-Rad, Hercules, CA). The purified 5′ end-labeled oligonucleotide was then added to CEM cells to a final concentration of 0.5 μM. Two aliquots of 1×10^6 cells each were taken at the beginning (time 0) and after 1, 2, and 4 h of incubation. At each time point, the cells were diluted with 10 volumes of ice-cold serum-free medium, and washed twice with the same volume of medium. The final pellet of the first aliquot of each sample was resuspended in 100 μL of a buffer containing 10 mM Tris-HCl, pH 7.4, and 10 mM EDTA (TE buffer) and used to determine the amount of ^{32}P-labeled oligonucleotide in whole cells by liquid scintillation counting. The second aliquot was processed to separate cytoplasm and nuclei. Cells were resuspended in 1 mL of a buffer containing 10 mM Tris-HCl, pH 7.4, 10 mM NaCl, 3 mM $MgCl_2$, and 0.5% (v/v) NP-40 (NP-40 buffer), incubated on ice for 5 min, and centrifuged at 500*g* at 4 °C for 5 min. The supernatants, representing the cytoplasmic fraction, were transferred to scintillation vials and counted. The pellets, which contained nuclei, were washed twice in NP-40 buffer. Nuclei in the final pellet were resuspended in 100 μL of TE buffer and transferred to scintillation vials for counting. Oligonucleotide concentrations in whole cells, cytoplasm, and nuclei were calculated on the basis of mean cell and nuclear volumes, which were determined on duplicate samples with a Coulter Counter Multisizer II (Beckman Coulter, Fullerton, CA). Aliquots (10 μL) of whole cells and nuclei were removed from each sample before counting and kept at −20 °C to determine the integrity of the ^{32}P-labeled oligonucleotide. To avoid further processing of the samples, each aliquot was directly diluted with an equal volume of denaturating gel loading buffer, heated at 95 °C for 5 min, and run on a 12% polyacrylamide sequencing gel.

Northern Blot. Total RNA was extracted by the guanidium isothiocyanate procedure (*42*). RNA concentrations were determined spectrophotometrically by measuring absorbance at 260 nm. Samples containing 5 μg of total RNA were electrophoresed on 1% agarose gel and transferred to nylon membranes (Magnagraph, MSI, Westboro, MA). *c-myc* and GAPDH cDNA were obtained from Oncor (Gaithersburg, MD) and American Type Culture Collection, respectively. Radiolabeled *c-myc* and GAPDH probes were prepared using a random priming kit (GIBCO/BRL) and purified with Biospin 30 columns (Bio-Rad). Hybridization of the blots with the ^{32}P-labeled probes and washing were carried out as previously described (*41*). After hybridization with the *c-myc* probe, the blots were washed and hybridized to the GAPDH probe to control for equal loading of RNA. The amounts of *c-myc* and GAPDH mRNA in each sample were determined by scanning the blots with a phosphoimager. The level of *c-myc* mRNA was then normalized for the amount of GAPDH mRNA to calculate the percentage of *c-myc* RNA in oligonucleotide-treated samples compared to untreated samples.

RT-PCR. Total RNA was prepared using the TRIzol reagent (GIBCO−BRL), and RT-PCR was performed using the SuperScript One-Step RT-PCR system (GIBCO−BRL) and gene-specific primers. In addition to the reagents present in the RT-PCR kit, each reaction contained 0.2 μM samples of *c-myc* primers (5′-TCGGAAGGACTATCCTGCTG-3′; 5′-GCTTTTGCTCCTCTGCTTGG-3′), a 0.15 μM aliquot of GAPDH primers (5′-GGGTGTGGGCAAGGTCATCC-3′;

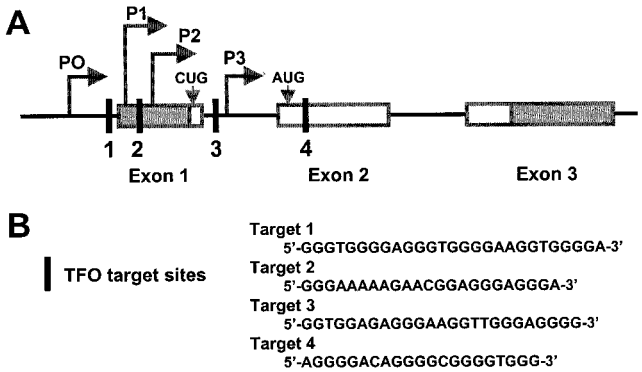

FIGURE 1: Organization of the *c-myc* gene and position of the TFO target sequences. (A) Map of the *c-myc* gene. Exons are represented by gray boxes with the translated portion in white. The translational start sites, CUG and AUG, are indicated by gray arrowheads. Gray arrows indicate the position of the transcription start sites. Black bars mark the position of the TFO target sites. (B) Nucleotide sequence of the purine-rich strands of the TFO target sites.

5′-TCCACCACCCTGTTGCTGTA-3′), and 100 ng of total RNA in a final volume of 50 μL. RT reactions were performed for 30 min at 50 °C, and were followed by 30 cycles of PCR (94 °C, 15 s; 55 °C, 30 s; 72 °C, 15 s) in a Pelkin Elmer 9600 thermal cycler. Samples were analyzed on 2% agarose gels and visualized by staining with ethidium bromide. The *c-myc* primers amplified a fragment of 292 bp in exon 3. GAPDH primers yielded a product of 332 bp. The intensity of the two bands in each sample was determined by densitometric analysis using the Gel-Pro Analyzer software (Media Cybernetics). Densitometric values relative to the *c-myc* band were normalized to those of the GAPDH to calculate the percentage of *c-myc* transcripts in oligonucleotide-treated cells compared to untreated control cells. Initial experiments were performed to optimize assay conditions (i.e., number of cycles, primer concentration, and amount of RNA template) in order to analyze *c-myc* and GAPDH transcripts in the exponential phase of amplification. The conditions described above yielded a linear relationship between the intensity of *c-myc* and GAPDH PCR products and the amount of RNA template added to the reaction.

RESULTS

Selection of Target Sites and Design of the TFOs. Figure 1 shows the position of the four sites selected for in vivo targeting of the endogenous *c-myc* gene by the triplex DNA-based approach. These target sites were chosen because they were either adjacent to critical regulatory elements or within the transcribed region of the gene. Therefore, oligonucleotide-directed triplex DNA formation at these sites was expected to block either transcription initiation or elongation of *c-myc* transcripts.

Site 1 is a 27 bp sequence located in the 5′ flanking region approximately 100 bp upstream of the P1 promoter. This sequence overlaps the binding site of various nuclear proteins known to activate *c-myc* transcription (*43*−*45*). TFOs directed to this site have been shown to inhibit transcription from the P1 promoter both in cell-free systems and in intact cells (*18*, *30*, *32*). Site 2 is a 23 bp sequence located in exon 1 immediately upstream of the P2 promoter, which is the major *c-myc* transcription start site (*3*). Binding sites for the transcription factors MAZ, E2F, and *ets* family members are positioned near this target sequence (*46*, *47*). TFOs directed to this sequence inhibit transcription initiation from the P2 promoter in vitro (*27*). More recently, TFOs directed to either site 1 or site 2 have been shown to inhibit expression of a luciferase reporter gene under the control of *c-myc* promoter sequences when cotransfected with the reporter gene construct (*28*). Sites 3 and 4 are located in intron 1 and exon 2, respectively. These sequences have not been targeted with TFOs before. Formation of triplex DNA at these sites, which are downstream of the major promoters, may prevent transcription elongation. Site 3 is also near the P3 promoter and regulatory elements, which are involved in initiation and regulation of *c-myc* transcription in some cell types (*3*, *48*).

The selected target sequences were all relatively purine-rich in one strand and pyrimidine-rich in the other, with only few pyrimidine interruptions in the purine-rich strands (Figure 1). Phosphodiester TFOs were designed to bind in antiparallel orientation to the purine-rich strand of the duplex DNA according to rules previously described in numerous studies (*10*−*12*). The sequence and length of the oligonucleotides are shown in Table 1. Most TFOs had G residues opposite GC base pairs, and T opposite AT base pairs, while T residues were placed opposite T and C bases interrupting the purine-rich sequences. This design was chosen because similar purine-rich or mixed purine/pyrimidine oligonucleotides had been shown to bind with high affinity and specificity to the target DNA at physiological pH (*10*−*12*). GA-rich TFOs directed to target sites 1 (myc1A) and 2 (myc2A), similar to TFOs used in previous studies (*18*, *27*, *28*, *30*), were also synthesized for comparison. Our studies showed that the GT-rich TFOs targeted to these two sites bound better than the corresponding GA-rich TFOs (see below). This is unlikely to be a general rule, since others

Table 1: Target Location, Sequence, and Size of TFOs Directed to the *c-myc* Gene

site	target location[a]	TFO	sequence	size
target 1	2180−2206	myc1	5′-TGGGGTGGTTGGGGTGGGTGGGGTGGG-3′	27
		myc1A	5′-TGGGGAGGTTGGGGAGGGTGGGGAGGG-3′	27
target 2	2427−2449	myc2	5′-TGGGTGGGTGGTTTGTTTTTGGG-3′	23
		myc2A	5′-AGGGAGGGAGGTAAGAAAAAGGG-3′	23
		myc2P	5′-GGGTTTTTGTTTGGTGGGTGGGT-3′	23
target 3	3959−3983	myc3	5′-GGGGTGGGTTGGTTGGGTGTGGTGG-3′	25
target 4	4689−4709	myc4	5′-GGGTGGGGTGGGGTTTGGGGT-3′	21
control 1	N/A	myc1M	5′-GGTGGGTGGGTGTGGGTGGGTGGGTGG-3′	27
control 2	N/A	myc2M	5′-GGTGTGTTGTTGGTGGTGTGTTG-3′	23

[a] Numbers correspond to the 5′ and 3′ nucleotides of the target sites according to the sequence of the human *c-myc* gene in GeneBank (HSMYCC locus).

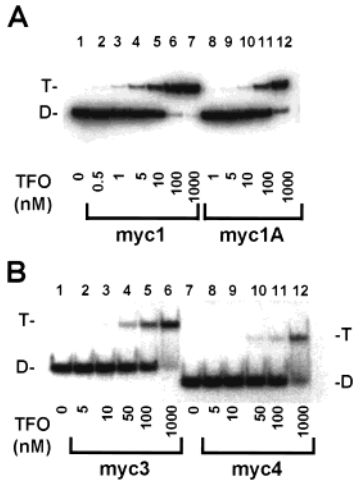

FIGURE 2: Electrophoretic mobility shift assays of triplex DNA formation by *c-myc*-targeting oligonucleotides. Oligonucleotides corresponding to the pyrimidine-rich strands of the target sites 1 (panel A) and 3 and 4 (panel B) in the *c-myc* gene were 5′ end-labeled with [γ-^{32}P]ATP and annealed to the complementary purine-rich oligonucleotides. Duplex DNA (1 nM) was incubated with the indicated TFOs in TBM buffer for 1 h at 37 °C. Samples were electrophoresed in a 12% nondenaturating polyacrylamide gel in TBM buffer at 600 V for 4 h. TFO concentrations are indicated below each lane. D and T, position of double- and triple-stranded DNA, respectively.

have shown equivalent or higher binding affinity of GA-rich compared to GT-rich TFOs (*49*, *50*).

Evaluation of Oligonucleotide-Directed Triplex DNA Formation. Binding of the *c-myc*-targeting TFOs to the corresponding target sequences was assessed by EMSA. In the experiments shown in Figure 2, TFOs were added at increasing concentrations to samples containing 1 nM of the corresponding radiolabeled duplex DNA and incubated for 1 h at 37 °C. Following this incubation, the samples were run on native polyacrylamide gels. Under nondenaturating conditions, triplex DNA would migrate more slowly than double-stranded DNA of identical size. Therefore, binding of a TFO to the target sequence would result in an upward shift of the band corresponding to the duplex DNA.

As shown in Figure 2 (panel A, lanes 2−7), myc1, which was directed to the site upstream of the P1 promoter, formed triplex DNA even at very low concentrations. A distinct band migrating more slowly than duplex DNA was detected at TFO concentrations as low as 1 nM (lane 3). Following incubation with 100 nM myc1 (i.e., 100-fold molar excess relative to target DNA), more than 90% of duplex DNA migrated as triplex DNA (lane 6). Analyzing data from multiple experiments, we determined that myc1 had a K_d of about 10^{-8} M. High binding affinities of similar GT-rich TFOs targeted to the P1 promoter site were also reported by Durland et al. (*40*). In contrast, Myc1A, which had A residues opposite the three TA base pairs in the target strand, was at least 10-fold less efficient than myc1 in this assay (Figure 2, panel A, lanes 8−12). A comparison of the results shown in Figure 2 with previously published data suggested that myc1 was also more efficient than another antiparallel GA-rich TFO, which was designed to target an alternative sequence in the P1 site (*28*). A complete shift of the duplex DNA was observed only when the concentration of this TFO was increased to 100 μM (equivalent to a 10 000-fold molar ratio of TFO to duplex DNA). EMSA was performed also with the mismatched oligonucleotide, myc1M, which had length and base composition similar to the TFOs, but different nucleotide sequence (see Table 1). Less than 3% of duplex DNA shifted to a higher position in the gel in the presence of 1 μM of the mismatched oligonucleotide (data not shown).

Similar EMSA studies were done by incubating the appropriate duplex DNA targets with various concentrations of the TFOs myc2, myc3, and myc4. As shown in panel B of Figure 2, both myc3 (lanes 2−6) and myc4 (lanes 8−12) formed triplex DNA that was detected as a distinct band migrating above that of the corresponding duplex DNA. Approximately 90% and 70% of duplex DNA migrated as triplex DNA in the presence of 1 μM aliquots of myc3 (lane 6) and myc4 (lane 12), respectively. Apparent K_d values for myc3 and myc4 were 1×10^{-7} and 4×10^{-7} M, respectively. Similar results with only 10−15% increases in the amount of triplex DNA were obtained when the TFOs myc1, myc3, and myc4 were incubated with the respective target sequences for 18 h before gel electrophoresis.

Binding of myc2 was more difficult to detect when EMSA was performed using the approach described above. Only a small upward shift of the duplex DNA band was observed in samples incubated with this TFO (data not shown). Although small, the shift was constantly reproduced in several experiments, in which various TFO concentrations, incubation times, and electrophoresis conditions were tested. To confirm the formation of triplex DNA by myc2, we performed additional EMSA studies, in which either the TFO or the control oligonucleotides were labeled instead of the duplex DNA target (*30*, *33*). We expected that the mobility shift generated upon binding of the single-stranded TFO to the duplex DNA target would be greater and easier to detect than with the previous approach. In the experiment shown in Figure 3 (panel A), myc2 (lanes 1−5), the mismatched oligonucleotide myc2M (lanes 6−10), and the parallel oligonucleotide myc2P (lanes 11−15) were end-labeled with ^{32}P and incubated with increasing concentrations of unlabeled duplex DNA. As shown in lanes 3 and 4, a clear upward shift was detected when samples containing 10 nM ^{32}P end-labeled myc2 were incubated with duplex DNA. More than 90% of myc2 migrated as triplex DNA in the presence of 0.5 and 1 μM duplex DNA (50- and 100-fold molar excess relative to the TFO). The estimated K_d values for myc2 in different experiments ranged from 5×10^{-8} to 1×10^{-7} M. As shown in Figure 3 (panel A, lanes 6−10), the mismatched oligonucleotide myc2M was unable to bind to the duplex DNA target under these conditions. Furthermore, the parallel oligonucleotide myc2P showed only a limited amount of binding ($\leq$5%) in the presence of 1 μM duplex DNA (lane 15), indicating that the preferential orientation of the third strand oligonucleotide was antiparallel to the purine-rich target strand. The results shown in Figure 3 suggested that myc2 had higher binding affinity than a GA-rich TFO used in previous studies (*27*, *28*). This TFO, which was identical to myc2A (Table 1), produced a complete shift of duplex DNA only at a concentration of 100 μM, which was equivalent to a 10 000-fold molar ratio of TFO to duplex DNA. When the experiment shown in Figure 3 was repeated with the ^{32}P end-labeled GA-rich TFO myc2A, we observed only a small amount of triplex DNA and the appearance of multiple bands at positions in the gel higher than that

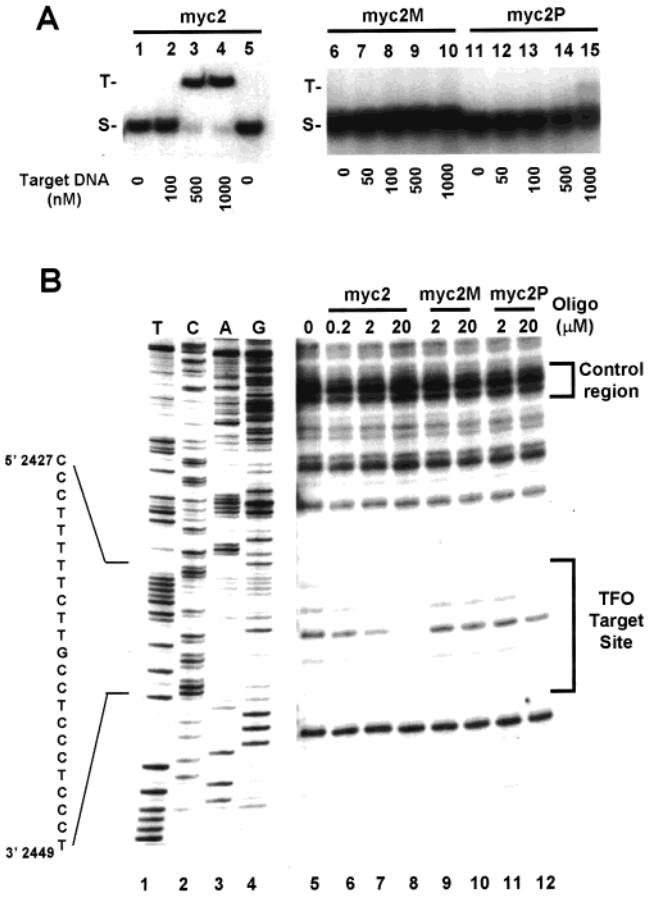

FIGURE 3: Oligonucleotide-directed triplex DNA formation at the target site upstream of the P2 promoter. (A) Electrophoretic mobility shift assay. Duplex DNA was prepared by annealing oligonucleotides corresponding to the pyrimidine- and purine-rich strands of target site 2. The oligonucleotides myc2 (lanes 1−5), myc2M (lanes 6−10), and myc2P (lanes 11−15) were 5′ end-labeled with [γ-^{32}P]-ATP and incubated at a final concentration of 10 nM with duplex DNA for 18 h at 37 °C. Samples were then separated on nondenaturating polyacrylamide gel as described in the legend to Figure 2. The concentrations of duplex DNA target are indicated below each lane. S and T, position of single- and triple-stranded DNA, respectively. (B) DNase I footprinting. A ^{32}P end-labeled DNA fragment containing the purine-rich target sequence upstream of the P2 promoter was incubated with myc2 (lanes 6−8), myc2M (lanes 9 and 10), and myc2P (lanes 11 and 12) for 24 h at 37 °C in TBM buffer. Oligonucleotide concentrations are indicated above each lane. Samples were then incubated with 10 units/mL DNase I for 1 min at room temperature and separated by electrophoresis on a 10% polyacrylamide gel. Sequencing reactions (T, C, A, and G in lanes 1−4) were run in adjacent lanes of the gel to determine the exact position of the target sequence. A shorter exposure of lanes 1−4 is shown for clarity. The pyrimidine-rich strand of the target sequence corresponding to nucleotides 2427−2449 in the *c-myc* gene is shown to the left of the panel. Brackets on the right side of the panel indicate the position of the TFO target site and a control region used for densitometric analysis.

expected for triplex DNA (data not shown). The tendency of myc2A, common to other GA-rich TFOs (*51*), to form aggregates might explain the decreased ability of this TFO to form triplex DNA and, perhaps, its reduced activity in cells (see below).

Binding of myc2 was also assessed by DNase I footprinting (Figure 3, panel B). In this assay, the products of a limited DNase I digestion are separated on a denaturating polyacrylamide gel and detected by autoradiography. A decrease of the intensity of the bands in a discrete region of the DNA ladder produced by DNase I would indicate protection from nucleolytic cleavage and identify the site of triplex DNA formation. A ^{32}P end-labeled fragment of the *c-myc* gene comprising the TFO target sequence upstream of the P2 promoter was incubated with either myc2 (lanes 6−8), myc2M (lanes 9 and 10), or myc2P (lanes 11 and 12) and subjected to DNase I digestion. As shown in Figure 3, a single protected region was observed in the 314 bp fragment following incubation with myc2. The protected region corresponded exactly to the 23 bp target sequence as determined by comparison with the adjacent sequencing ladder. Protection of the target sequence was concentration-dependent with apparently complete protection at 20 μM myc2 (lane 8). Similar results were obtained in separate experiments, in which mapping of the TFO binding site was done by DMS footprinting (data not shown). To determine more precisely the extent of DNase I protection achieved with various concentrations of myc2, the intensity of bands within the target sequence was measured by densitometry. Bands in a region outside the target sequence were used as control to correct for any difference in sample loading. About 20, 50, and 95% of the target sequence was protected from DNase I in samples containing 0.2, 2, and 20 μM myc2, respectively. In contrast, incubation with 2 and 20 μM myc2M did not cause any protection of the target sequence or any other site within the 314 bp DNA fragment (lanes 9 and 10). Some protection of the target sequence (20%) was detected in the samples incubated with 20 μM myc2P (lane 12). Therefore, DNase I footprinting confirmed the results obtained with EMSA and demonstrated sequence-specific binding of myc2 to the target site.

Cellular Uptake and Stability of 3′-Amino-Modified Oligonucleotides. Cell permeability, nuclear localization, and stability of the oligonucleotides are primary concerns for the use of TFOs in tissue culture experiments and in vivo applications. A number of studies have shown that the stability of phosphodiester oligonucleotides can be improved by modifying their 3′ terminus with the addition of a propylamine group (*22*, *31*, *52*). This modification reduces the susceptibility of the oligonucleotides to exonuclease degradation, and, therefore, is expected to increase their stability and activity in biological systems. Furthermore, 3′-amino-modified oligonucleotides are able to form triplex DNA with an affinity for the target sequence identical to that of unmodified TFOs (data not shown).

The following studies were done to determine uptake, distribution, and stability of 3′-amino-modified phosphodiester oligonucleotides in human leukemia CEM cells. To carry out these studies, the 3′A-TFO myc1A was 5′ end-labeled with ^{32}P, purified, and then added to cells to a final concentration of 0.5 μM. Aliquots of cells were removed at the indicated time points and processed to determine the amount of ^{32}P-labeled 3′A-TFO in whole cells, cytoplasm, and nuclei. Figure 4 shows a plot of the oligonucleotide concentrations achieved in each cell compartment during the 4 h incubation. There was significant uptake of the oligonucleotide in these cells, with intracellular concentrations rapidly exceeding that in the extracellular medium. Furthermore, higher concentrations of the 3′A-TFO were present at each time point in nuclei compared to cytoplasm and whole cells, indicating a rapid accumulation of the oligonucleotide in this cell compartment. To determine the physical state of

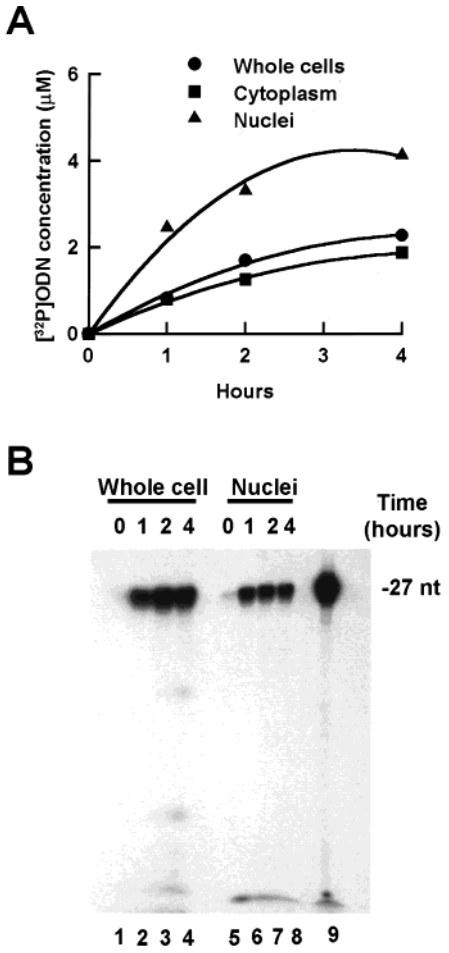

FIGURE 4: Uptake and stability of a 3′-amino-modified oligonucleotide in human leukemia CEM cells. (A) Uptake and intracellular distribution of a 3′-amino-TFO. CEM cells were incubated with 0.5 μM ^{32}P-labeled myc1A. Aliquots of 1×10^6 cells were taken at the indicated time points and processed to measure the amount of ^{32}P-labeled oligonucleotide in whole cells, cytoplasm, and nuclei. Oligonucleotide concentrations in each cell compartment were calculated on the basis of mean cellular (1350 μm^3) and nuclear (254 μm^3) volumes determined with a cell counter. (B) Stability of a 3′-amino-TFO in whole cells and nuclei. Ten microliter aliquots of whole cells (lanes 1−4) and nuclei (lanes 5−8) were diluted in denaturating loading buffer, heated at 95 °C for 5 min, and loaded on a 12% denaturating polyacrylamide gel. Lane 9, ^{32}P-labeled 3′A-myc1A used as size marker.

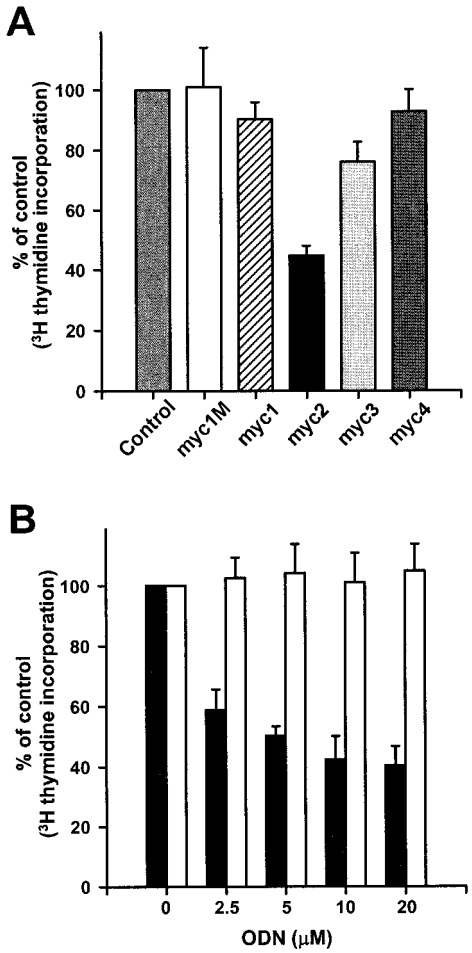

FIGURE 5: Effects of *c-myc*-targeting TFOs on proliferation of human T-cell leukemia CEM cells. (A) Cells (5×10^4/mL) were incubated with 10 μM aliquots of the indicated oligonucleotides for 96 h. [^{3}H]Thymidine was added to the culture medium during the last 24 h of the incubation. Following TCA precipitation on GF/C filters, liquid scintillation counting was used to measure the amount of [^{3}H]thymidine incorporated at the end of the incubation. (B) Cells were incubated with increasing concentrations of either myc2 (black bars) or the mismatched oligonucleotide myc1M (white bars) for 96 h and processed as described above. In both panels, the results are expressed as percentage of [^{3}H]thymidine incorporated in oligonucleotide-treated cells compared to untreated control cells. Triplicate samples were analyzed in each experiment, and the data shown in each panel are means ± SD of the results of two separate experiments.

the oligonucleotide, aliquots of cells and nuclei were directly lysed in denaturating gel loading buffer and analyzed by gel electrophoresis. This method avoided any additional processing of the samples, which could compromise recovery of the oligonucleotide and analysis of its degradation profile (*30*). As shown in panel B of Figure 4, more than 95% of the ^{32}P end-labeled 3′A-TFO was intact in whole cells and nuclei at the end of the 4 h incubation. Thus, these results confirmed the ability of human leukemia cells in culture to take up oligonucleotides and the relative intracellular stability of 3′A-TFOs. Particularly relevant to the use of oligonucleotides in a triplex DNA-based approach is the extent of nuclear accumulation of intact 3′A-TFO seen in these cells.

Antiproliferative Activity of c-myc-Targeting TFOs in Human T-Cell Leukemia Cells. The *c-myc* gene product is an important regulator of cell growth and differentiation (*1*). Downregulation of *c-myc* gene expression and function is associated with inhibition of cell proliferation in a variety of cancer cell types, including human leukemia and lymphoma cells (*4*−*9*). To evaluate the biological activity of the *c-myc*-targeting TFOs and their potential as cancer therapeutic agents, we measured their ability to inhibit the growth of human leukemia CEM cells. These T-cell leukemia cells express high levels of *c-myc* in the absence of gene amplification or chromosomal translocation, and downregulation of *c-myc* expression in these cells is associated with growth arrest and cell death (*53*). Our hypothesis was that TFOs that were able to bind to critical sites in the *c-myc* gene and inhibit its expression would have a direct inhibitory effect on the proliferation of these cells.

CEM cells were incubated with the TFOs for 96 h. During the last 24 h of incubation, radiolabeled thymidine was added to the culture medium. The cells were then harvested to measure the amount of thymidine incorporated into cellular DNA. Figure 5 (panel A) shows the degree of cell growth

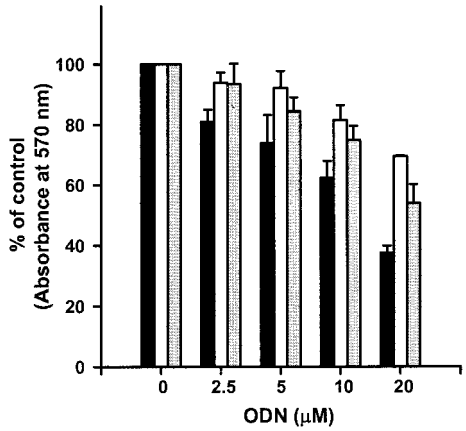

FIGURE 6: Effects of the TFOs myc2 and myc3 and the parallel control oligonucleotide myc2P on growth and viability of CEM cells. Cells (5×10^4/mL) were incubated with myc2 (black bars), myc2P (white bars), and myc3 (gray bars). The number of viable cells following a 96 h incubation was determined by the MTT assay. The absorbance at 570 nm was measured with a microplate reader, and the results are expressed as a percentage of absorbance in oligonucleotide-treated samples relative to untreated samples. Triplicate samples were analyzed in each experiment, and the data shown are means ± SD of the results of two separate experiments.

inhibition observed in cells incubated with 10 μM samples of various TFOs and a control oligonucleotide as a percentage of thymidine incorporation in untreated control cells. Myc2, which is directed to the site immediately upstream of the P2 promoter (site 2 in Figure 1), was the most effective inhibitor of cell proliferation. This TFO reduced thymidine incorporation to 45 ± 3% ($P < 0.00001$) compared to both untreated control cells and cells treated with the mismatched oligonucleotide myc1M. Myc3 had a smaller effect on cell growth (76 ± 5% of control, $P < 0.001$), while myc1 and myc4 did not have statistically significant effects on the growth of CEM cells. The antiproliferative activity of myc2 and the specificity of its effects were confirmed by incubating CEM cells in the presence of various concentrations of this TFO and the mismached oligonucleotide myc1M (Figure 5, panel B). Myc2 at concentrations ranging from 2.5 to 20 μM inhibited cell proliferation. In contrast, cell growth was not affected by exposure of the cells to identical concentrations of the mismatched oligonucleotide.

Comparable results were obtained when cell number and viability were assessed by the MTT assay. Figure 6 shows the results of an experiment in which the effects of the TFOs myc2 and myc3 and the parallel oligonucleotide myc2P were evaluated using this assay. Following a 96 h incubation, myc2 induced a dose-dependent decrease in the number of viable cells with a 60% reduction at 20 μM compared to the untreated control cells. Both myc2P and myc3 were less effective than myc2, reducing cell viability by 20 and 40% compared to control cells, respectively. Other oligonucleotides, including myc1, myc1A, myc1M, myc2A, and myc2M, were assayed and did not have any significant effect on cell viability (data not shown). This confirmed that the GT-rich TFO myc2, which targeted the P2 promoter site, was the most effective TFO in these cells. It should also be noted that, particularly at concentrations lower than 10 μM, the effects on cell viability assessed by the MTT assay were less pronounced than those on cell proliferation measured by the thymidine incorporation assay. This suggested that inhibition of cell proliferation by the *c-myc*-targeting TFO preceded loss of cell viability.

Taken together, these results indicated that *c-myc*-targeting TFOs had antiproliferative activity in human leukemia cells. The effects depended on the position of the target site relative to regulatory elements in the gene, since the TFO directed to a sequence immediately upstream of the P2 promoter was more effective than TFOs targeted to any other site in the *c-myc* promoter or coding region. Considering that mismatched and parallel control oligonucleotides did not have any significant effect on cell growth and that the other TFOs had length, nucleotide composition, and in vitro binding affinity very similar to myc2, our results argued strongly in favor of the sequence-specificity of the effects of this TFO.

Inhibition of c-myc Gene Expression by the myc2 TFO. The effects of myc2 were sequence-dependent, arguing for a specific triplex DNA-mediated mechanism leading to inhibition of *c-myc* gene expression and cell growth by this TFO. To provide direct evidence of the involvement of selective inhibition of *c-myc* expression, we measured *c-myc* mRNA levels in untreated control cells and cells incubated for 4 h with various TFOs and control oligonucleotides. As shown in Figure 7 (panel A), the level of *c-myc* mRNA, assessed by Northern blot, was reduced by about 50% in cells treated with 20 μM myc2 compared to untreated control cells. The levels of GAPDH mRNA as well as the amounts of the 18S and 28S ribosomal RNA species were identical in the two samples, indicating equal RNA loading. The effects of myc2, other TFOs, and control oligonucleotides on *c-myc* mRNA levels were further examined by RT-PCR. In the experiments shown in panels B−D of Figure 7, GAPDH-specific primers were used along with *c-myc*-specific primers in the same reaction tube so that the amount of *c-myc* product in each sample could be normalized to that of this housekeeping gene. As shown in panel B, the levels of *c-myc* mRNA in cells treated with 5, 10, and 20 μM myc2 were 85, 76, and 57%, respectively, compared to the level in untreated control cells. Unlike myc2, other TFOs and control oligonucleotides did not affect *c-myc* gene expression significantly at concentrations of 10 and 20 μM (panels C and D, respectively). Therefore, inhibition of cell growth by myc2 was associated with and, apparently, dependent on the ability of this TFO to inhibit *c-myc* gene expression. On the other hand, the lack of effect of other TFOs and control oligonucleotides on cell growth could be explained by their inability to affect *c-myc* gene expression.

Antiproliferative Activity of c-myc-Targeting TFOs in Acute Myeloid Leukemia and Burkitt's Lymphoma Cells. Further studies were carried out to determine the effects of TFOs targeted to selected sites in the *c-myc* gene on the growth of various leukemia and lymphoma cell lines. The major goal of these studies was to determine whether the observations made in CEM cells regarding the antiproliferative activity of the myc2 TFO could be extended to cells of different origin and with different mechanisms of activation of *c-myc* gene expression. These studies provided also an opportunity to test the selectivity of the triplex DNA-based approach by comparing the antiproliferative effects of TFOs directed to distinct sites in the gene in cells, such as Burkitt's lymphoma cells, with known structural alterations in the *c-myc* locus.

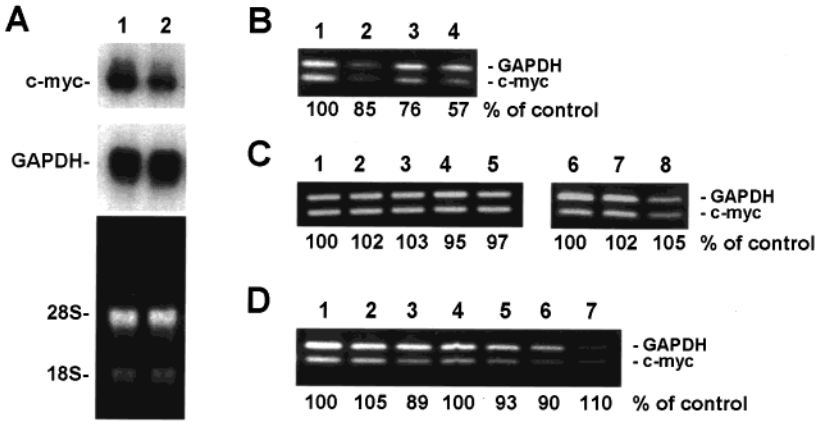

FIGURE 7: Downregulation of *c-myc* gene expression by the myc2 TFO in human leukemia cells. CEM cells were incubated with the indicated oligonucleotides for 4 h. RNA was extracted, and *c-myc* mRNA levels were determined by either Northern blot (panel A) or RT-PCR (panels B−D). For Northern analysis, total RNA was separated on a 1% agarose gel and transferred to a nylon membrane, which was then hybridized to radiolabeled *c-myc* and GAPDH probes. The ethidium bromide-stained gel is shown to confirm equal RNA loading. For RT-PCR, total RNA was reverse-transcribed and amplified with *c-myc* and GAPDH-specific primers. PCR products were separated on 2% agarose gels and visualized by ethidium bromide staining. The level of GAPDH product was used as internal control for the efficiency of the RT-PCR and sample loading. In each sample, the intensity of the *c-myc* band was normalized to the intensity of the GAPDH band to determine the level of *c-myc* transcripts. Percent values relative to untreated control cells are shown below each lane. Panel A: lane 1, untreated control cells; lane 2, cells incubated with 20 μM myc2. Panel B: lane 1, untreated control cells; lanes 2−4, cells incubated with 5, 10, and 20 μM myc2, respectively. Panel C: lanes 1 and 6, untreated control cells; lanes 2−5, cells incubated with 10 μM myc2M, myc1T, myc1M, and myc3T, respectively; lanes 7 and 8, cells incubated with 10 μM myc2A and myc2P, respectively. Panel D: lane 1, untreated control cells; lanes 2−7, cells incubated with 20 μM myc2M, myc1T, myc1M, myc2A, myc3T, and myc2P, respectively.

Two AML cell lines, KG-1 and HL-60, and two Burkitt's lymphoma cell lines, Raji and ST486, were used in these studies. KG-1 cells do not have amplification or rearrangements involving the *c-myc* gene. Like the majority of AML cells, KG-1 cells express *c-myc* in response to either autocrine or paracrine stimulation by growth factors, such as GM-CSF (*54*). HL-60 cells have amplification of the *c-myc* gene (*55*). Amplification, however, does not change the organization of the *c-myc* regulatory region, and the P2 promoter still serves as the major transcription start site in these cells. Therefore, both AML cell lines were expected to be sensitive to the TFO targeting the P2 promoter site. Figure 8 shows the effects of the TFOs myc2 and myc3 and the parallel control oligonucleotide myc2P on KG-1 and HL-60 cell growth. Incubation for 96 h with 20 and 25 μM myc2 inhibited the growth of KG-1 and HL-60 cells, respectively, by approximately 50%. At these concentrations, myc3 and myc2P were less effective than myc2 in both cell lines. These results were very similar to those obtained with the same oligonucleotides in CEM cells (see Figure 6). The greater sensitivity of these cells to myc2 compared to myc3 apparently reflected the importance of the corresponding target regions for *c-myc* gene expression. We determined by RT-PCR that the *c-myc* mRNA level was reduced in both HL-60 and KG-1 cells by at least 30% following a 4 h incubation with 20 μM myc2, but was not affected by an identical concentration of myc3 (data not shown). It is worth noting that myc2 completely inhibited the growth of HL-60 cells at a concentration of 50 μM, whereas the control oligonucleotide myc2P induced only 10−15% of growth inhibition. At this high concentration, myc3 was able to inhibit the growth of HL-60 cells by about 80%. The activity of the myc3 TFO in HL-60 cells may be related to the presence of regulatory elements in intron 1, which are apparently important for control of *c-myc* gene expression in these cells (*48*).

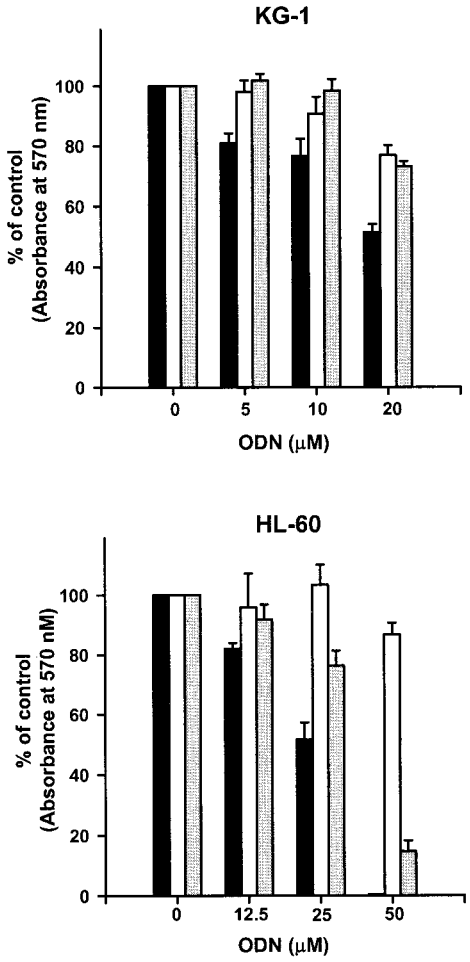

FIGURE 8: Effects of *c-myc*-targeting TFOs on the growth of human acute myeloid leukemia cells. KG-1 and HL-60 cells were incubated with myc2 (black bars), myc2P (white bars), and myc3 (gray bars) at the indicated concentrations. The number of viable cells was determined after 96 h by the MTT assay as described in the legend to Figure 6. Top panel, KG-1 cells; bottom panel, HL-60 cells.

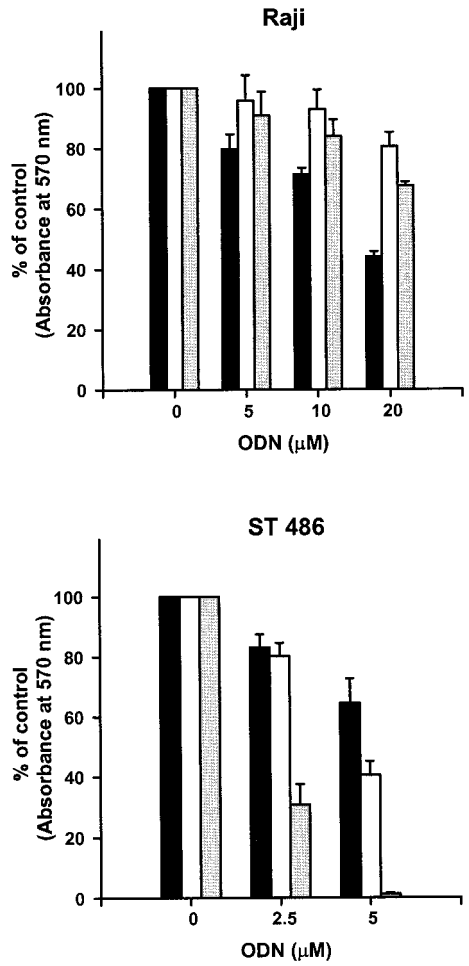

FIGURE 9: Effects of TFOs targeted to distinct sites in the *c-myc* promoter on the growth of Burkitt's lymphoma cells. Raji and ST486 cells were incubated with myc2 (black bars), myc2P (white bars), and myc3 (gray bars) and the number of viable cells was determined after 96 h by the MTT assay as described in the legend to Figure 6. Top panel, Raji cells; bottom panel, ST486 cells.

Figure 9 shows results obtained with the B-cell lymphoma cell lines, Raji and ST486. In both cell lines, one allele of the *c-myc* gene is translocated to chromosome 14, as commonly observed in Burkitt's lymphomas (*3*). Expression of the translocated allele is constitutively activated by enhancer sequences derived from the immunoglobulin locus on chromosome 14, whereas the untranslocated allele is silenced. Raji and ST486 cells, however, differ in the position of the chromosomal breakpoint relative to the *c-myc* transcription unit, and this results in critical differences in the organization of the gene regulatory region and promoter usage (*56*, *57*). The site of the breakpoint is upstream of exon 1 in Raji cells, while it occurs within the first intron in ST486 cells (see Figure 1). Therefore, the P1 and P2 promoters and the regulatory elements in exon 1 of the translocated allele are intact and functional in Raji cells (*57*). In contrast, the translocated *c-myc* gene lacks exon 1 in ST486 cells, and its transcription initiates at the P3 promoter site located in intron 1. As shown in Figure 9, results similar to those obtained with CEM, KG-1, and HL-60 cells were observed when Raji cells were incubated with myc2, myc3, and myc2P. Myc2 inhibited cell growth by about 50% at a concentration of 20 μM, whereas myc3 and myc2P decreased cell growth by only 30 and 15%, respectively. The ability of myc2 to inhibit the growth of Raji cells was consistent with the fact that the t(8;14) chromosomal translocation did not affect the region that included the myc2 target site. The reduced sensitivity of Raji cells to myc3 compared to myc2 was also consistent with the fact that the P2 promoter remained the major transcription start site in these cells.

In ST486 cells, as a result of the translocation, the regulatory and promoter sequences in exon 1 are separated from the rest of the gene (*56*). These elements, including the myc2 target sequence, are still present in the untranslocated allele and in the portion of the translocated allele remaining on chromosome 8. However, they do not play a role in transcription of the translocated *c-myc* gene. Unlike the situation in Raji cells, therefore, oligonucleotide-directed triplex DNA formation at the myc2 site would not be expected to interfere with *c-myc* expression. Since transcription in the translocated allele starts from the P3 promoter, however, *c-myc* expression and, consequently, ST486 cell growth might be affected by myc3, whose binding sequence is immediately upstream of the P3 promoter in intron 1. According to this hypothesis, therefore, ST486 cells would be expected to be more sensitive to myc3 than myc2. Figure 9 shows that myc3 inhibited the growth of ST486 cells by about 70% at a concentration of 2.5 μM. In contrast, myc2 and myc2P at the same concentration inhibited cell growth by only 17 and 20% compared to untreated control cells. At a concentration of 5 μM, both myc2 and myc2P had significant effects on cell growth (35 and 55% inhibition, respectively). However, at this concentration, myc3 inhibited almost completely ST486 cell growth (99% inhibition). Therefore, in agreement with our initial hypothesis, myc3 was much more effective than myc2 at all concentrations tested, probably reflecting the greater activity of the P3 promoter in these cells. We also isolated total RNA from ST486 cells, either untreated or treated with TFOs, and measured the level of *c-myc* mRNA by RT-PCR. Myc3 at 2.5 μM reduced *c-myc* mRNA by about 30% in ST486 cells, whereas myc2 did not affect *c-myc* expression at this concentration (data not shown).

DISCUSSION

The present study demonstrates the antiproliferative activity of 3′-amino-modified phosphodiester TFOs designed to act as selective repressors of *c-myc* gene expression in human leukemia and lymphoma cells. Although there have been several reports on the ability of TFOs to inhibit transcription of reporter gene constructs, only few studies have shown inhibition of endogenous gene expression (*30*−*37*) and cell proliferation (*34*, *37*, *38*) by a triplex DNA-based approach in cell culture experiments. Herein, we show that a GT-rich TFO directed to a site immediately upstream of the P2 promoter of the *c-myc* gene inhibits gene expression and cell proliferation in human leukemia CEM cells. Reduction of *c-myc* protein level by other means has been shown to result in cell growth arrest, differentiation, and death in many cancer cell types (*4*, *5*, *7*, *58*−*61*). In fact, using a nuclease-resistant phosphorothioate TFO similar to myc2, we have recently shown that downregulation of *c-myc* expression in CEM cells is associated with inhibition of cell cycle progression and induction of apoptotic cell death (*62*). The effects of the myc2 TFO on gene expression and cell proliferation are both sequence- and target-specific. Mis-

matched and parallel control oligonucleotides do not affect *c-myc* gene expression and cell growth. Furthermore, TFOs directed to other sites in the *c-myc* gene are less or not active. This suggests a high degree of selectivity and sequence-specificity of the triplex DNA-based approach, since all the TFOs used in this study are very similar in length, base composition, and in vitro binding affinity. Indeed, some of the TFOs are inactive despite the presence of G-rich sequence elements (e.g., G quartets) which are known as a potential source of nonspecific effects (*63*).

Further evidence of the specificity and potential selectivity of the triplex DNA-based approach comes from the observation that the relative sensitivity of various cell lines to TFOs targeting distinct sites in exon 1 (myc2) and intron 1 (myc3) depends on both the presence and the function of the respective target sequences. To the best of our knowledge, this is the first study in which the effects of TFOs have been evaluated in cells that have distinct alterations of the endogenous target gene in the attempt to test the selectivity of this approach. Myc2 is more active than myc3 in cells, such as CEM, KG-1, HL-60, and Raji, in which the region comprising its target site is intact. As discussed below, we believe that this is due to the particular relevance of this region for the activity of the P2 promoter, which is the major *c-myc* promoter in these cells. In contrast, ST486 cells are considerably more sensitive to myc3 than myc 2. In these Burkitt's lymphoma cells, the t(8;14) chromosomal translocation causes the separation of exon 1 from the rest of the gene, thereby eliminating the P2 promoter and activating the P3 promoter in the translocated allele (*56*). Because of the position of the myc3 target site, which is immediately upstream of the P3 promoter in intron 1, it is possible that this TFO acts by repressing transcription initiation in the translocated and constitutively active *c-myc* allele. However, there is yet no direct evidence of a role of the myc3 target sequence in P3 promoter activity. Also unclear are the mechanisms underlying the growth inhibitory activity of myc2 and myc2P at high concentrations in ST486 cells. This may be due to nonspecific and non-triplex-mediated effects of the oligonucleotides. However, the effects of myc2 and myc2P seem to be sequence-specific, since the mismatched oligonucleotide myc2M had only minimal effects on the growth of ST486 cells at similar concentrations (data not shown). In light of the fact that myc2 target sequences are still present in the translocated and untranslocated allele, one cannot rule out the possibility that these effects might be due to triplex-mediated binding to the target sequence and induction of secondary events leading to cell growth inhibition. In addition, the portion of the translocated *c-myc* allele that remains on chromosome 8 is actively transcribed, and high levels of short transcripts containing exon 1 sequences and with unknown function are present in ST486 cells (*56*).

Even though we do not provide direct evidence of triplex DNA formation at the target site in cells, the effects of the myc2 TFO on gene expression and cell proliferation shown in this study are likely due to inhibition of transcription by a triplex DNA-mediated mechanism. Studies in a cell-free system have shown that targeting the region upstream of the P2 promoter with a similar TFO blocks transcription from this initiation site (*27*). This conclusion is also supported by our observation that TFOs and control oligonucleotides that have similar base composition but are unable to form triplex DNA with the specific target sequence do not inhibit *c-myc* gene expression and cell growth. Moreover, an important aspect of the design of our GT-rich TFOs is that their sequences are not identical or complementary to either strand of the corresponding target sequences. This greatly reduces the chances of sequence-specific interactions of the TFOs with single-stranded DNA, RNA, or single-stranded DNA binding proteins. Such interactions may theoretically lead to inhibition of *c-myc* gene expression at a transcriptional or translational level by either an antisense or a decoy-like mechanism. The possibility of these alternative mechanisms has raised concerns about the real nature of the biological effects of TFOs described in earlier studies (*18, 30, 38*). A decoy-like mechanism has been invoked as a possible explanation of the inhibition of *c-myc* gene expression by a TFO, which was directed to the site upstream of the P1 promoter (*18, 30, 38*). Unlike the TFOs used in our study, this TFO was identical to the purine-rich strand of the target site both in sequence and in orientation. It was later shown that this parallel, purine-rich TFO could bind CNBP, a sequence-specific single-stranded DNA binding protein that activates *c-myc* transcription (*44*). The interaction of the purine-rich oligonucleotide with this trans-activating factor was suggested as a possible cause of transcriptional inhibition induced by the TFO in cell-free systems and cells. More recently, it has been proposed that this purine-rich TFO might also hybridize to the complementary pyrimidine-rich strand of the target DNA (*64*). This would prevent binding of another *c-myc* transcriptional activator, hnRNP K, which specifically interacts with the pyrimidine-rich single-stranded DNA sequence, thus resulting in transcriptional inhibition (*64*). Interestingly, we have not detected inhibition of endogenous *c-myc* gene expression and cell growth by the antiparallel GT-rich TFO myc1, which is also directed to the P1 promoter site and forms triplex DNA with very high binding affinity. As for the TFO targeting the P2 promoter site, further studies are certainly required to determine whether sequence-specific, non-triplex-mediated mechanisms have any role in the inhibition of gene expression and cell growth induced by this TFO. Our studies with myc2A and myc2P, which have sequences very similar to myc2, however, suggest that interactions of the TFO with *c-myc* promoter elements or sequence-specific single-stranded DNA binding proteins are unlikely to be involved in myc2 activity. Myc2A has only one mismatch compared to the purine strand of the myc2 target sequence. In contrast, myc2 has 11 nucleotide mismatches relative to the purine strand and 12 mismatches relative to the pyrimidine strand. Furthermore, myc2P has a sequence identical to myc2, only with opposite orientation. If sequence-specific interactions occurred and were indeed responsible for non-triplex-mediated effects, one would expect that myc2A and myc2P would have similar or even greater activity than myc2. However, both these oligonucleotides have no or minimal activity in our assays.

The greater activity of myc2 compared to other TFOs may be due in part to the importance of the cis-elements adjacent to its target site for regulation of *c-myc* expression. The P2 promoter is the major transcription start site responsible for 75−90% of *c-myc* transcripts (*3*). The region targeted by myc2 overlaps regulatory elements that are critical for P2 promoter activity, and deletions in this region result in loss

of transcriptional activity (*46*, *47*). In contrast, triplex DNA formation at sites other than the P2 promoter site may have a less disruptive effect on *c-myc* expression. TFOs targeted to the myc1 site have been shown to inhibit predominantly transcription from the P1 promoter (*18*, *30*), which is, however, responsible for only 10−25% of *c-myc* transcripts (*3*). Therefore, even complete inhibition of P1 promoter activity may not be sufficient to reduce significantly *c-myc* levels in cells. Similar considerations may apply to the TFOs myc3 and myc4, which are directed to sites downstream of the major *c-myc* promoters. Although triplex DNA formation downstream of a transcription start site has been shown to inhibit transcription elongation (*19*, *25*), this mechanism may be less effective in cells than inhibition of transcription initiation by a TFO directed to a promoter sequence. Interestingly, the same TFO, myc3, which has limited activity in most cell lines tested, is active in ST486 cells where it is probably acting as an inhibitor of transcription initiation from the P3 promoter site.

Accessibility of the target sequence is another factor that may contribute to differences in the activity of the *c-myc*-targeting TFOs. Measurements of the binding affinity to target DNA in vitro do not show significant differences among TFOs. However, the sequences targeted by TFOs other than myc2 may be less accessible or suitable for triplex DNA formation in cells than the myc2 binding site. This may be a plausible explanation of the lack of effect of the P1 targeting TFO myc1. The region targeted by this TFO has been shown to undergo complex conformational changes that, in addition to double-stranded DNA, involve an equilibrium between single-stranded and tetraplex DNA (*64*, *65*). DNA in these alternative conformations would not bind a TFO. In addition, proteins, such as CNBP and hnRNP K, which bind to either the purine or the pyrimidine strand of the target sequence have been identified (*44*, *45*). Binding of these proteins may also prevent oligonucleotide-directed triplex DNA formation. In apparent contrast with this explanation, an antiparallel GT-rich TFO targeted to the sequence upstream of the P1 promoter has been shown to inhibit *c-myc* expression in MCF7 cells (*32*). The TFO used in that study was 37 nucleotides long and affected *c-myc* expression only when it was administered along with a synthetic polyamine known to stabilize triplex DNA. Therefore, it is possible that the increased length of the TFO and the presence of a triplex-stabilizing compound might have facilitated triplex DNA formation in cells. This also suggests that modifications of oligonucleotide design or the use of triplex-stabilizing agents may overcome obstacles to triplex DNA formation related to DNA conformation or site accessibility and increase the potency of TFOs.

One of the challenges of research in oncology is to find ways to utilize the increasing knowledge of the mechanisms underlying neoplastic transformation and tumor progression to develop novel therapeutic strategies for cancer. Targeting specific genes, such as *c-myc*, which are involved in proliferation and survival of cancer cells is a promising approach. Our study shows the ability of TFOs designed to target *c-myc* promoter sequences to downregulate gene expression and inhibit proliferation of human leukemia and lymphoma cells. Future studies will need to establish the efficacy of this approach in vivo.

ACKNOWLEDGMENT

We thank Charlene Alford, Department of Biochemistry and Molecular Biology, Medical University of South Carolina, for her assistance with oligonucleotide synthesis, and Drs. D. Watson and A. Safa for the gift of KG-1, Raji, and HL-60 cells.

REFERENCES

1. Dang, C. V. (1999) *Mol. Cell. Biol. 19*, 1−11.
2. Nesbit, C. E., Tersak, J. M., and Prochownik, E. V. (1999) *Oncogene 18*, 3004−3016.
3. Spencer, C. A., and Groudine, M. (1991) *Adv. Cancer Res. 56*, 1−48.
4. Holt, J. T., Redner, R. L., and Nienhuis, A. W. (1988) *Mol. Cell. Biol. 8*, 963−973.
5. Wickstrom, E. L., Bacon, T. A., Gonzalez, A., Freeman, D. L., Lyman, G. H., and Wickstrom, E. (1988) *Proc. Natl. Acad. Sci. U.S.A. 85*, 1028−1032.
6. McManaway, M. E., Neckers, L. M., Loke, S. L., al-Nasser, A. A., Redner, R. L., Shiramizu, B. T., Goldschmidts, W. L., Huber, B. E., Bhatia, K., and Magrath, I. T. (1990) *Lancet 335*, 808−811.
7. Kimura, S., Maekawa, T., Hirakawa, K., Murakami, A., and Abe, T. (1995) *Cancer Res. 55*, 1379−1384.
8. Sawyers, C. L., Callahan, W., and Witte, O. N. (1992) *Cell 70*, 901−910.
9. Bourgeade, M. F., Defachelles, A. S., and Cayre, Y. E. (1998) *Blood 91*, 3333−3339.
10. Helene, C., and Toulme, J. J. (1990) *Biochim. Biophys. Acta 1049*, 99−125.
11. Maher, L. J., III (1996) *Cancer Invest. 14*, 66−82.
12. Chan, P. P., and Glazer, P. M. (1997) *J. Mol. Med. 75*, 267−282.
13. Beal, P. A., and Dervan, P. B. (1991) *Science 251*, 1360−1363.
14. Beal, P. A., and Dervan, P. B. (1992) *Nucleic Acids Res. 20*, 2773−2776.
15. Singleton, S. F., and Dervan, P. B. (1992) *Biochemistry 31*, 10995−11003.
16. Maher, L. J. d., Wold, B., and Dervan, P. B. (1989) *Science 245*, 725−730.
17. Maher, L. J. d., Dervan, P. B., and Wold, B. (1992) *Biochemistry 31*, 70−81.
18. Cooney, M., Czernuszewicz, G., Postel, E. H., Flint, S. J., and Hogan, M. E. (1988) *Science 241*, 456−459.
19. Young, S. L., Krawczyk, S. H., Matteucci, M. D., and Toole, J. J. (1991) *Proc. Natl. Acad. Sci. U.S.A. 88*, 10023−10026.
20. Grigoriev, M., Praseuth, D., Robin, P., Hemar, A., Saison-Behmoaras, T., Dautry-Varsat, A., Thuong, N. T., Helene, C., and Harel-Bellan, A. (1992) *J. Biol. Chem. 267*, 3389−3395.
21. Grigoriev, M., Praseuth, D., Guieysse, A. L., Robin, P., Thuong, N. T., Helene, C., and Harel-Bellan, A. (1993) *Proc. Natl. Acad. Sci. U.S.A. 90*, 3501−3505.
22. Ing, N. H., Beekman, J. M., Kessler, D. J., Murphy, M., Jayaraman, K., Zendegui, J. G., Hogan, M. E., O'Malley, B. W., and Tsai, M. J. (1993) *Nucleic Acids Res. 21*, 2789−2796.
23. Ebbinghaus, S. W., Gee, J. E., Rodu, B., Mayfield, C. A., Sanders, G., and Miller, D. M. (1993) *J. Clin. Invest. 92*, 2433−2439.
24. Mayfield, C., Ebbinghaus, S., Gee, J., Jones, D., Rodu, B., Squibb, M., and Miller, D. (1994) *J. Biol. Chem. 269*, 18232−18238.
25. Rando, R. F., DePaolis, L., Durland, R. H., Jayaraman, K., Kessler, D. J., and Hogan, M. E. (1994) *Nucleic Acids Res. 22*, 678−685.
26. Reddoch, J. F., and Miller, D. M. (1995) *Biochemistry 34*, 7659−7667.
27. Kim, H. G., and Miller, D. M. (1995) *Biochemistry 34*, 8165−8171.
28. Kim, H. G., Reddoch, J. F., Mayfield, C., Ebbinghaus, S., Vigneswaran, N., Thomas, S., Jones, D. E., Jr., and Miller, D. M. (1998) *Biochemistry 37*, 2299−2304.

29. Kim, H. G., and Miller, D. M. (1998) *Biochemistry 37*, 2666−2672.
30. Postel, E. H., Flint, S. J., Kessler, D. J., and Hogan, M. E. (1991) *Proc. Natl. Acad. Sci. U.S.A. 88*, 8227−8231.
31. Orson, F. M., Thomas, D. W., McShan, W. M., Kessler, D. J., and Hogan, M. E. (1991) *Nucleic Acids Res. 19*, 3435−3441.
32. Thomas, T. J., Faaland, C. A., Gallo, M. A., and Thomas, T. (1995) *Nucleic Acids Res. 23*, 3594−3599.
33. Tu, G. C., Cao, Q. N., and Israel, Y. (1995) *J. Biol. Chem. 270*, 28402−28407.
34. Aggarwal, B. B., Schwarz, L., Hogan, M. E., and Rando, R. F. (1996) *Cancer Res. 56*, 5156−5164.
35. Porumb, H., Gousset, H., Letellier, R., Salle, V., Briane, D., Vassy, J., Amor-Gueret, M., Israel, L., and Taillandier, E. (1996) *Cancer Res. 56*, 515−522.
36. Kochetkova, M., and Shannon, M. F. (1996) *J. Biol. Chem. 271*, 14438−14444.
37. Kochetkova, M., Iversen, P. O., Lopez, A. F., and Shannon, M. F. (1997) *J. Clin. Invest. 99*, 3000−3008.
38. Helm, C. W., Shrestha, K., Thomas, S., Shingleton, H. M., and Miller, D. M. (1993) *Gynecol. Oncol. 49*, 339−343.
39. Calabretta, B., and Skorski, T. (1997) *Anti-Cancer Drug Des. 12*, 373−381.
40. Durland, R. H., Kessler, D. J., Gunnell, S., Duvic, M., Pettitt, B. M., and Hogan, M. E. (1991) *Biochemistry 30*, 9246−9255.
41. Catapano, C. V., Carbone, G. M., Pisani, F., Qiu, J., and Fernandes, D. J. (1997) *Biochemistry 36*, 5739−5748.
42. Chomczynski, P., and Sacchi, N. (1987) *Anal. Biochem. 162*, 156−159.
43. Postel, E. H., Mango, S. E., and Flint, S. J. (1989) *Mol. Cell. Biol. 9*, 5123−5133.
44. Michelotti, E. F., Tomonaga, T., Krutzsch, H., and Levens, D. (1995) *J. Biol. Chem. 270*, 9494−9499.
45. Michelotti, E. F., Michelotti, G. A., Aronsohn, A. I., and Levens, D. (1996) *Mol. Cell. Biol. 16*, 2350−2360.
46. Bossone, S. A., Asselin, C., Patel, A. J., and Marcu, K. B. (1992) *Proc. Natl. Acad. Sci. U.S.A. 89*, 7452−7456.
47. Roussel, M. F., Davis, J. N., Cleveland, J. L., Ghysdael, J., and Hiebert, S. W. (1994) *Oncogene 9*, 405−415.
48. Pan, Q., and Simpson, R. U. (1999) *J. Biol. Chem. 274*, 8437−8444.
49. Chandler, S. P., and Fox, K. R. (1996) *Biochemistry 35*, 15038−15048.
50. Perkins, B. D., Wilson, J. H., Wensel, T. G., and Vasquez, K. M. (1998) *Biochemistry 37*, 11315−11322.
51. Noonberg, S. B., Francois, J. C., Garestier, T., and Helene, C. (1995) *Nucleic Acids Res. 23*, 1956−1963.
52. Zendegui, J. G., Vasquez, K. M., Tinsley, J. H., Kessler, D. J., and Hogan, M. E. (1992) *Nucleic Acids Res. 20*, 307−314.
53. Thulasi, R., Harbour, D. V., and Thompson, E. B. (1993) *J. Biol. Chem. 268*, 18306−18312.
54. Schwartz, E. L., Chamberlin, H., and Brechbuhl, A. B. (1991) *Blood 77*, 2716−2723.
55. Collins, S., and Groudine, M. (1982) *Nature 298*, 679−681.
56. ar-Rushdi, A., Nishikura, K., Erikson, J., Watt, R., Rovera, G., and Croce, C. M. (1983) *Science 222*, 390−393.
57. Taub, R., Moulding, C., Battey, J., Murphy, W., Vasicek, T., Lenoir, G. M., and Leder, P. (1984) *Cell 36*, 339−348.
58. Watson, P. H., Pon, R. T., and Shiu, R. P. (1991) *Cancer Res. 51*, 3996−4000.
59. Collins, J. F., Herman, P., Schuch, C., and Bagby, G. C., Jr. (1992) *J. Clin. Invest. 89*, 1523−1527.
60. Skorski, T., Nieborowska-Skorska, M., Campbell, K., Iozzo, R. V., Zon, G., Darzynkiewicz, Z., and Calabretta, B. (1995) *J. Exp. Med. 182*, 1645−1653.
61. Leonetti, C., D'Agnano, I., Lozupone, F., Valentini, A., Geiser, T., Zon, G., Calabretta, B., Citro, G. C., and Zupi, G. (1996) *J. Natl. Cancer Inst. 88*, 419−429.
62. McGuffie, E. M., Carbone, G. M. R., Pacheco, D., and Catapano, C. V. (1999) *Proc. AACR 19*, 130.
63. Stein, C. A. (1996) *J. Natl. Cancer Inst. 88*, 391−393.
64. Simonsson, T., Pecinka, P., and Kubista, M. (1998) *Nucleic Acids Res. 26*, 1167−1172.
65. Michelotti, G. A., Michelotti, E. F., Pullner, A., Duncan, R. C., Eick, D., and D., L. (1996) *Mol. Cell. Biol. 16*, 2656−2669.

BI992185W